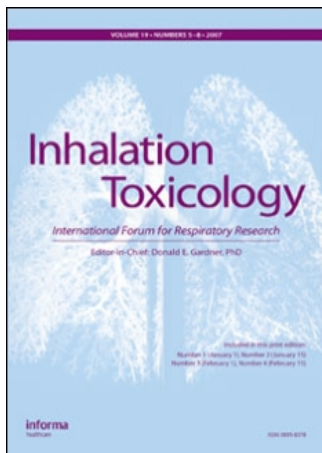


This article was downloaded by:[University of Leicester]
On: 12 June 2008
Access Details: [subscription number 773557640]
Publisher: Informa Healthcare
Informa Ltd Registered in England and Wales Registered Number: 1072954
Registered office: Mortimer House, 37-41 Mortimer Street, London W1T 3JH, UK



Inhalation Toxicology

International Forum for Respiratory Research

Publication details, including instructions for authors and subscription information:
<http://www.informaworld.com/smpp/title~content=t713657711>

Comparison of Calidria Chrysotile Asbestos to Pure Tremolite: Final Results of the Inhalation Biopersistence and Histopathology Examination Following Short-Term Exposure

David M. Bernstein ^a; Jörg Chevalier ^b; Paul Smith ^c

^a Consultant in Toxicology, Geneva, Switzerland

^b EPS Experimental Pathology Services AG, Muttenz, Switzerland

^c Research & Consulting Company Ltd., Füllinsdorf, Switzerland

Online Publication Date: 01 August 2005

To cite this Article: Bernstein, David M., Chevalier, Jörg and Smith, Paul (2005) 'Comparison of Calidria Chrysotile Asbestos to Pure Tremolite: Final Results of the Inhalation Biopersistence and Histopathology Examination Following Short-Term Exposure', *Inhalation Toxicology*, 17:9, 427 — 449

To link to this article: DOI: 10.1080/08958370591002012

URL: <http://dx.doi.org/10.1080/08958370591002012>

PLEASE SCROLL DOWN FOR ARTICLE

Full terms and conditions of use: <http://www.informaworld.com/terms-and-conditions-of-access.pdf>

This article maybe used for research, teaching and private study purposes. Any substantial or systematic reproduction, re-distribution, re-selling, loan or sub-licensing, systematic supply or distribution in any form to anyone is expressly forbidden.

The publisher does not give any warranty express or implied or make any representation that the contents will be complete or accurate or up to date. The accuracy of any instructions, formulae and drug doses should be independently verified with primary sources. The publisher shall not be liable for any loss, actions, claims, proceedings, demand or costs or damages whatsoever or howsoever caused arising directly or indirectly in connection with or arising out of the use of this material.

Comparison of Calidria Chrysotile Asbestos to Pure Tremolite: Final Results of the Inhalation Biopersistence and Histopathology Examination Following Short-Term Exposure

David M. Bernstein

Consultant in Toxicology, Geneva, Switzerland

Jörg Chevalier

EPS Experimental Pathology Services AG, Muttenz, Switzerland

Paul Smith

Research & Consulting Company Ltd., Füllinsdorf, Switzerland

Calidria chrysotile asbestos, which is a serpentine mineral, has been shown to be considerably less biopersistent than the durable amphibole mineral tremolite asbestos, which persists once deposited in the lung. The initial results of this inhalation biopersistence study in rats that demonstrates this difference were reported in Bernstein et al. (2003). This article presents the full results through 1 yr after cessation of the 5-day exposure. This study was based upon the recommendations of the European Commission (EC) Interim Protocol for the Inhalation Biopersistence of synthetic mineral fibers (Bernstein & Riego-Sintes, 1999). In addition, the histopathological response in the lung was evaluated following exposure. In order to quantify the dynamics and rate by which these fibers are removed from the lung, the biopersistence of a sample of commercial-grade chrysotile from the Coalinga mine in New Idria, CA, of the type Calidria RG144 and that of a long-fiber tremolite were studied. For synthetic vitreous fibers, the biopersistence of the fibers longer than 20 μm has been found to be directly related to their potential to cause disease. This study was designed to determine lung clearance (biopersistence) and the histopathological response. As the long fibers have been shown to have the greatest potential for pathogenicity, the aerosol generation technique was designed to maximize the number of long respirable fibers. The chrysotile samples were specifically chosen to have 200 fibers/cm³ longer than 20 μm in length present in the exposure aerosol. These longer fibers were found to be largely composed of multiple shorter fibrils. The tremolite samples were chosen to have 100 fibers/cm³ longer than 20 μm in length present in the exposure aerosol. Calidria chrysotile has been found to be one of the most rapidly cleared mineral fibers from the lung. The fibers longer than 20 μm in length are cleared with a half-time of 7 h. By 2 days postexposure all long fibers have dissolved/disintegrated into shorter pieces. The fibers between 5 and 20 μm in length were cleared with a half-time of 7 days. This length range represents a transition zone between those fibers that can be fully phagocytosed and cleared as particles and the longer fibers that cannot be fully engulfed by the macrophage. The fibers/objects shorter than 5 μm in length were cleared with a half-time of 64 days, which is faster than that reported for insoluble nuisance dusts such as TiO₂. By 12 months postexposure, 99.92% of all the remaining chrysotile was less than 5 μm in length. Following the 5 days of repeated exposure to more than 48,000 chrysotile fibers/cm³ (190 fibers L > 20 μm), histopathological examination revealed no evidence of any inflammatory reaction either after the cessation of the last exposure or at any time during the subsequent 12-mo period. This is in marked contrast to the amphibole tremolite, which was also investigated using the same inhalation biopersistence protocol. The long tremolite fibers, once deposited in the lung, remain over the rat's lifetime with essentially an infinite half-time. Even

Received 6 January 2005; accepted 25 February 2005.

This research was sponsored by a grant from the Union Carbide Corporation.

Address correspondence to Dr. David M. Bernstein, Consultant in Toxicology, 40 chemin de la Petite-Boissière, 1208 Geneva, Switzerland.

E-mail: davidb@itox.ch

the shorter fibers, following early clearance, also remain with no dissolution or further removal. At 365 days postexposure, there was a mean lung burden was of 0.5 million fibers $L > 20 \mu\text{m}$ and 7 million fibers $5\text{--}20 \mu\text{m}$ in length with a total mean lung burden of 19.6 million fibers. The tremolite exposed rats, even with exposure to 16 times fewer total fibers than chrysotile, showed a pronounced inflammatory response with the rapid development of granulomas as seen at day 1 postexposure, followed by the development of fibrosis characterized by collagen deposition within these granulomas and by 90 days even mild interstitial fibrosis. With the short exposure, this study was not designed specifically to evaluate pathological response; however, it is quite interesting that even so there was such a marked response with tremolite. These findings provide an important basis for substantiating both kinetically and pathologically the differences between chrysotile and the amphibole tremolite. As Calidria chrysotile has been certified to have no tremolite fiber, the results of the current study together with the results from toxicological and epidemiological studies indicate that this fiber is not associated with lung disease.

The marked difference in biopersistence between the serpentine mineral chrysotile asbestos and the amphibole asbestos such as amosite and tremolite has now been demonstrated in studies of three different chrysotiles (Bernstein et al., 2003, 2004, 2005). While all chrysotiles have been shown to clear quickly from the lung, the Calidria chrysotile clears the fastest, with a clearance half-time of the fibers longer than $20 \mu\text{m}$ of 7 h. These results were initially presented as interim results based upon measurements through 90 days after cessation of exposure (Bernstein et al., 2003). This publication presents the results of the inhalation biopersistence studies of both Calidria chrysotile and tremolite through the full 12 mo postexposure. Presented as well are the results from the histopathological examination of both chrysotile and tremolite through the same time period.

METHODS

Chrysotile and Tremolite Sample Characteristics

The chrysotile studied was obtained from the Coalinga mine in New Idria, CA, of the commercial product Calidria type RG144, and was produced by Union Carbide. This is the same type of chrysotile evaluated by Muhle et al. (1987a) and Ilgren and Chatfield (1997, 1998a, 1998b, 2002) and that was found not to produce excess tumours following chronic inhalation in rats. Chrysotile samples from the same mine have been analyzed for purity using chemical separation procedures to concentrate and extract fibers other than chrysotile. The results of this examination of samples from both mining and processing operations revealed that the only asbestos mineral detectable was chrysotile and that no tremolite was present in the asbestos from this mine (Pooley, 2003; Coleman, 1996).

The tremolite sample was obtained from Dr. Alan Jones of the Institute of Occupational Medicine, Edinburgh, Scotland. Davis et al. (1985) evaluated a similar sample in a chronic inhalation study in rats and found that rats treated with tremolite developed very high levels of pulmonary fibrosis as well as 16 carcinomas and 2 mesotheliomas in a group of 39 animals.

The differences between the serpentine chrysotile and the amphiboles such as amosite, crocidolite, and tremolite have already been presented in detail. The chemical composition of the amphiboles fibers is more complex than that of chrysotile. The

idealized chemical formulas of different types of amphiboles are shown next. This variability in composition is a direct consequence of the fact that the structure can accommodate many different ions in the space between the silica ribbons, which form the fibers, and that the variable nature of the host rocks can contribute different ions to this structure (Speil & Leineweber, 1969).

Crocidolite: $(\text{Na}_2\text{Fe}_3^{2+}\text{Fe}_2^{3+}) \text{Si}_8\text{O}_{22}(\text{OH})_2$

Amosite: $(\text{Fe}^{2+}, \text{Mg})_7 \text{Si}_8\text{O}_{22}(\text{OH})_2$

Tremolite: $\text{Ca}_2\text{Mg}_5 \text{Si}_8\text{O}_{22}(\text{OH})_2$

Anthophyllite: $(\text{Mg}, \text{Fe}^{2+})_7 \text{Si}_8\text{O}_{22}(\text{OH})_2$

Actinolite: $\text{Ca}_2(\text{Mg}, \text{Fe}^{2+})_5 \text{Si}_8\text{O}_{22}(\text{OH})_2$

While magnesium is an important part of both chrysotile (~33%) and amphiboles such as tremolite (~25%), in chrysotile the magnesium molecule is on the outside of the curled chrysotile structure. This is of particular importance in that magnesium is soluble in the lung fluids and can be readily leached from the surface. With amphiboles such as tremolite, the magnesium is locked within the I-beam type structure, which consists of corner-linked $(\text{SiO}_4)^4$ tetrahedra linked together in a double-tetrahedral chain that sandwiches a layer with the Ca_2Mg_5 .

Fibrous chrysotile has been shown as well to be acid soluble in contrast to the amphiboles. Hargreaves and Taylor (1946) reported that if fibrous chrysotile is treated with dilute acid the magnesia can be completely removed. The hydrated silica that remains, though fibrous in form, had completely lost the elasticity characteristic of the original chrysotile and gave an x-ray pattern of one or perhaps two diffuse broad bands, indicating that the structure is "amorphous" or "glassy" in type. This difference in characteristics is also important in the lung, where the macrophage is capable of generating a milieu at a pH of ~4.5. Badollet (1948, 1951) summarized the available information on the stability of asbestiform minerals. He reported that strong acids decompose chrysotile rapidly with the removal of all MgO and a total weight loss of 60%. The residue that remains after acid attack consists of amorphous silica, which retains a very fragile fibrous morphology.

Chrysotile is also decomposed by water. Reimschuessel (1969) studied the extraction of chrysotile with boiling water. He reported that after an initial rapid reaction, magnesium and silica

are removed from the chrysotile in amounts proportional to the chrysotile concentration. Speil and Leineweber (1969) reported that these results show that there is no doubt that chrysotile is slowly soluble in water under conditions of continuous extraction.

Most important, however, is that chrysotile is a sheet silicate. That is, instead of forming in rods (fibers) as do the amphiboles, it forms in thin sheets. These sheets, however, have a mineral composition such that the spacing between the magnesium ions is greater than that between the silica ions. This mismatch in spacing causes the chrysotile to curl into effectively a rolled fiber. This is illustrated in Figure 1.

Most chrysotile asbestos ores consist of chrysotile in the form of cross- or slip-fiber veins within massive serpentinite rock, which has to be mined to be extracted. This format is almost absent from the New Idria body from which Calidria chrysotile is obtained. Instead, the ore consists of friable masses of matted chrysotile surrounded by fragments of serpentinite rock. The ore is highly sheared and pulverized and sits freely on the surface, which allowed mining to be carried out by simple collection methods with the production of high-quality asbestos by straightforward wet or dry separation processes. The Coalinga ore deposit contains more than 50% chrysotile, in contrast to the <10% recoverable fiber in typical cross- or slip-fiber ores (Mumpton & Thompson, 1975).

Amphiboles, such as tremolite, are double-chain silicates. Figure 2A shows the amphiboles schematically with the slice directly across the chains.

Each of the blue boxes represents a double chain of tetrahedral (SiO_2). (The tetrahedra are illustrated in the middle chains.) With tremolite, the white and green circles represent the magnesium and calcium cations that effectively glue one chain to its neighbor.

Fewer shared cations bond the chains together along the broad sides of the chains compared to the narrow sides, resulting in these broad surfaces being bonded less strongly. As shown in Figure 2B it is along these weakly bonded surfaces, shown in red dashed lines, that the mineral will most likely break. With tremolite, these weak bonds are associated with the Mg. Figure 2C simplifies the picture and shows that the double-chain silicates can break into a set of fragments with potentially regular shape.

Figure 2D shows the same situation in 3 dimensions. The potential breakages run along the chains and it can be seen how the fiber shape is formed. The chains themselves do not break easily because the bonds between the silica tetrahedra are very strong compared to the bonds gluing one chain to the next.

Experimental Design

The experimental design of the in-life and biopersistence analysis has been presented in detail previously (Bernstein et al., 2003) and is summarized next. In particular, details of the counting and sizing procedures are reiterated, as these are considered essential to the successful interpretation of these studies.

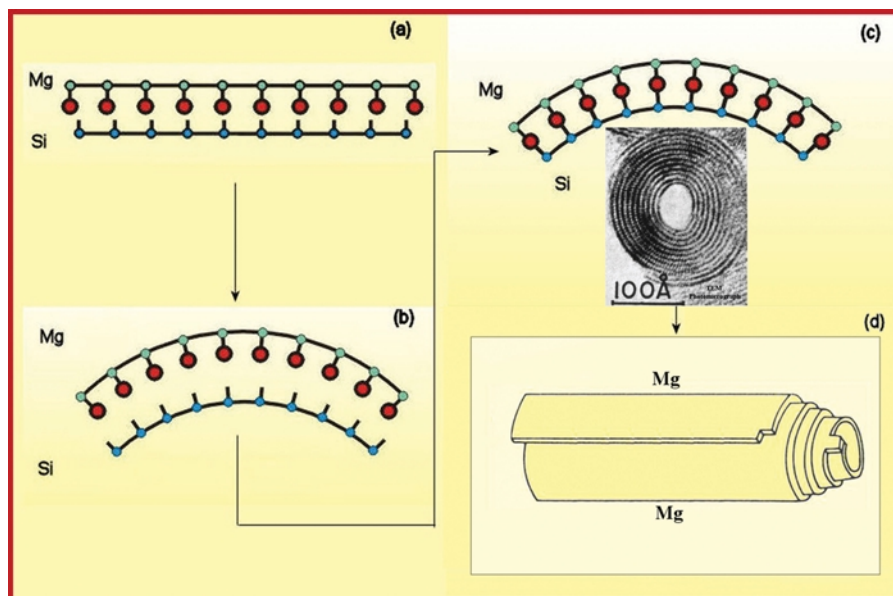


FIG. 1. Structural formation of the sheet silica chrysotile asbestos. Schematic representation of the structural formation of the sheet silica chrysotile asbestos, showing the positioning of the Mg molecule on the outside of the curl. (A) Relative spacing of the Mg and Si sheets. (B) How the sheets have to curl in order for the Mg and Si atoms to line up. Also shown is a transmission electron micrograph of the cross section of a chrysotile fiber showing the curled structure. (C) How this results in chrysotile being formed as a rolled fiber (D). Adapted with permission from http://academic.brooklyn.cuny.edu/geology/powell/core_asbestos/asbestoshome.htm.

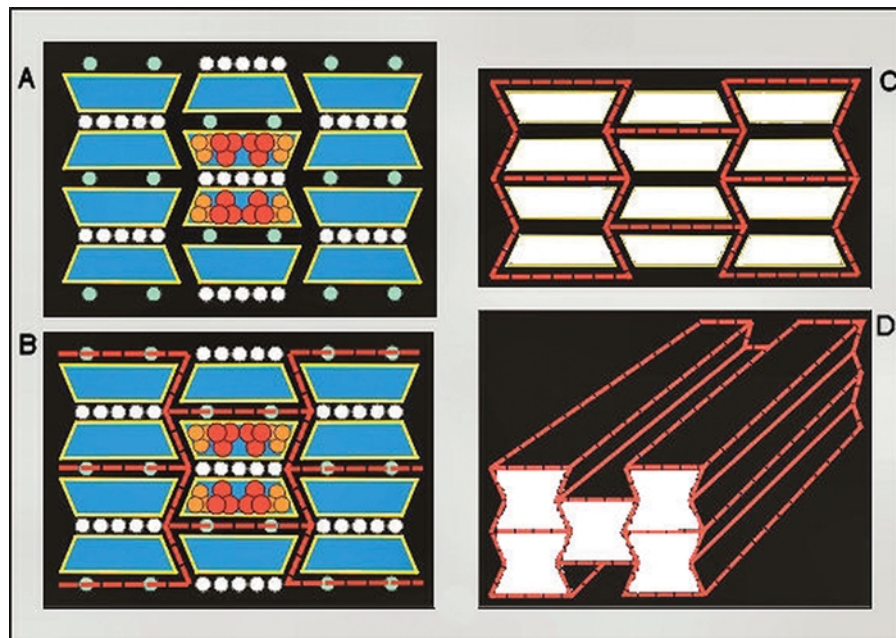


FIG. 2. Structural formation of the double-chain silica tremolite asbestos. The structural formation of the double chain silica tremolite asbestos. (A) Amphiboles schematically, with the slice directly across the chains. Each of the blue boxes represents a double-chain of tetrahedral (SiO_2). (The tetrahedra are illustrated in the middle chains.) With tremolite, the white and green circles represent the magnesium and calcium cations that glue one chain to its neighbour. Fewer shared cations bond the chains together along the broad sides of the chains compared to the narrow sides. These broad surfaces are, therefore, bonded less strongly. (B) It is along these weakly bonded surfaces, shown in red dashed lines, that the mineral will most likely break. With tremolite, these weak bonds are associated with the Mg. (C) Simplified picture showing that the double-chain silicates can break into a set of fragments with potentially regular shape. (D) The same situation in three dimensions. The potential breakages run along the chains and it can be seen how the fiber shape is formed. The chains themselves do not break easily because the bonds between the silica tetrahedra are very strong compared to the bonds gluing one chain to the next.

Animal Exposure. Groups of 56 weanling (~ 8 wk old) male rats were exposed by flow-past nose-only exposure to a target fiber aerosol concentration for the Calidria chrysotile of 200 fibers $L > 20 \mu\text{m}/\text{cm}^3$ and for tremolite of 100 fibers $L > 20 \mu\text{m}/\text{cm}^3$ for 6 h/day for a period of 5 consecutive days. A chrysotile concentration twice that required by the EC Biopersistence Protocol (Bernstein & Riego-Sintes, 1999) was used in order to assure that there was no question of sufficient long fiber exposure. In addition, a negative control group was exposed in a similar fashion to filtered air. To be comparable with current and previous fiber inhalation studies, Wistar rats (HanBrl:WIST, specific-pathogen-free) were used that were obtained from RCC Ltd, Biotechnology and Animal Breeding Division, Füllinsdorf, Switzerland.

Exposure System. The fiber aerosol generation system was designed to loft the bulk fibers without breaking, grinding, or contaminating the fibers (Bernstein et al., 1994). The animals were exposed by the flow-past nose/snout-only inhalation exposure system. This system was derived from Cannon et al. (1983) and is different from conventional nose-only exposure systems in that fresh fiber aerosol is supplied to each animal individually and exhaled air is immediately exhausted.

Fiber Clearance. At 0 days (immediately after the cessation of exposure), 1 day, 2 days, 7 days, 2 wk, 1 mo, 3-mo, 6 mo, and 12 mo postexposure, the lungs from subgroups of animals were weighed and then digested by low-temperature plasma ashing and subsequently analyzed by transmission electron microscopy (at the GSA Corp.) for total chrysotile fibers number in the lungs and chrysotile fiber size (length and diameter) distribution in the lungs.

Clinical Examination and Body Weights. All animals were observed for mortality/morbidity twice daily, prior to and following exposure and at least once daily during the acclimatization period and the 12-mo observation period. Clinical signs were recorded during the 5-day exposure period twice daily, prior to and following exposure, and after cessation of exposure once weekly during the month and every second week thereafter. All animals were sacrificed by exsanguination following deep anesthesia by intraperitoneal injection of sodium pentobarbital (approximately 300 mg/kg). Each animal was weighed on day 1 (used for randomization) and day 8 of the acclimatization period, on days 1, 3, and 5 of the exposure period, once weekly during the month following the last day of exposure and every second week thereafter.

Histopathology. At 1, 2, 14, and 90 days and at 6 and 12 mo, separate subgroups of animals were taken for histopathological examination of the respiratory tract. At necropsy, the lungs were weighed and then the left lobe of the lung of each animal was inflated through a bronchial cannula with a neutral buffered 4% formaldehyde solution (formalin). The mediastinal lymph nodes were also fixed in formalin. The lung and lymph nodes were processed, embedded in paraffin, cut at a nominal thickness of 2–4 μm and stained with hematoxylin and eosin for histopathological examination. In addition, sections of the lung were also stained with Masson's trichrome for collagen evaluation. All abnormalities were described and reported and gross observations were when possible correlated with microscopic findings. The remaining lung lobes were preserved by Rogers Imaging Company (Needham, MA) for optional examination by confocal microscopy.

In the scoring system used for individual pathologic diagnoses, the histological changes were described according to distribution, severity, and morphologic character. The severity was scored as minimal, slight, moderate, marked, or massive (grades 1–5, respectively).

Lung Digestion for Fiber/Particle Analysis. From 5 rats per group per time point the lungs were frozen at necropsy at -20°C . The frozen lungs were subsequently dehydrated by freeze drying (Edwards EF4 Modulyo freeze-dryer) and dried to constant weight to determine the dry weight of the tissue. The dry tissue was plasma ashed in a Plasma systems 200 (Technics Plasma GmbH) for at least 16 h. Upon removal from the ashing unit, the ash from each lung was weighed and suspended in 10 ml methanol using a low-intensity ultrasonic bath. The suspension was then transferred into a glass bottle with the combustion boat rinse and the volume made up to 20 ml. An aliquot was then removed and filtered onto a gold-coated polycarbonate filter (pore size of 0.2 μm).

Counting Rules for the Evaluation of Air and Lung Samples by Transmission Electron Microscopy. All fibers visible at a magnification of 10,000 \times were taken into consideration. All objects seen at this magnification were sized with no lower or upper limit imposed on either length or diameter. The bivariate length and diameter was recorded individually for each object measured. Fibers were defined as any object that had an aspect ratio of at least 3:1. The diameter was determined at the greatest width of the object. All other objects were considered as nonfibrous particles.

The stopping rules for counting of each sample were defined as follows: For nonfibrous particles, the recording of particles was stopped when a total of 30 particles were recorded. For fibers, the recording was stopped when 500 fibers with length $\geq 5 \mu\text{m}$, diameter $\leq 3 \mu\text{m}$ (often referred to as WHO Fibers; WHO, 1987) or a total of 1000 fibers and nonfibrous particles were recorded. If this number of fibers was not reached after evaluation of 0.15 mm^2 of filter surface, additional fields of view were counted until either 500 WHO fibers was reached or a total of 5 mm^2 of filter surface was evaluated, even if a total

of 500 countable WHO fibers was not reached. The evaluation of objects of length $< 5 \mu\text{m}$ was stopped when 100 objects were reached.

Validation of the Lung Digestion and Counting Procedures. The validity of the results reported depends upon validation that the lung digestion and counting procedures did not significantly alter the fiber length distribution.

The only method suitable for validation of chrysotile fiber recovery would be a parallel analysis using a nonevasive measurement technique such as confocal microscopy (Bernstein et al., 2004, 2005). To validate the procedures, the lungs from 3 rats exposed at the same time and under the same conditions as mentioned and sacrificed at 1 day after cessation of exposure were analyzed.

At necropsy the lungs were removed and were fixed in Karnovsky's fixative by gentle instillation under a pressure of 30 cm H_2O with simultaneous immersion in fixative. The trachea was then ligated and the inflated lungs were stored in the same fixative. Following fixation, apical lobes were divided into 5 pieces (10 $\text{mm}^2 \times 5 \text{mm}$ thick) cut parallel to the hilum, dehydrated in graded ethanolic series to absolute, stained with 0.005% Lucifer yellow, and embedded in Spurr plastic for microscopic analysis (Rogers et al., 1999). Flat surfaces were prepared from hardened plastic blocks containing embedded lung pieces.

Confocal microscopy was performed on three randomly selected animals from each time point using Sarastro 2000 (Molecular Dynamics, Inc.) laser scanning microscopes fitted with 25-mW argon-ion lasers and an upright microscope (Optiphot-2; Nikon, Inc., or Zeiss Axiophot) modified for reflected-light imaging. These confocal microscopes were used to record image data in dual channel reflected and fluorescent imaging mode. Optical bench settings for the Sarastro 2000 CLSMs were: excitation 488 nm (Lucifer yellow), emission 488 nm notch ($\pm 2 \text{nm}$) and a 510 long-pass filter, laser power 12–15 mW, 30% transmission, photomultiplier voltage set between 500–800 V. Fluorescently labeled cellular constituents and reflective/refractive fibers (and particles) were imaged simultaneously with this arrangement. Each "exposure" produced two digital images in perfect register with one another.

An image recorded in either mode was a two-dimensional (x, y), 512 \times 512 array of pixels, each with an intensity value from 0 to 254 gray-scale units (a value of 255 indicated saturation of the intensity scale). Optical (x, y) sections, individually and in depth series, were recorded at various positions along the z axis by adjusting the stage height using stepper motors under computer control. Images and image series were analyzed and prepared for presentation by employing specialized computer software. Images were recorded through 40 \times objectives. The dimensions of pixels in the recorded volume were (x, y , and z dimensions, respectively) 0.13 μm , 0.13 μm , and 0.3 μm .

Our procedure was to place the microscope objective at random over the lung specimen exposed at the surface of the epoxy embedment, collect a depth series of images, return to the initial

starting depth, move two field widths in the positive x direction, and repeat the process. Twenty five depth series per piece of lung (for a total of 100 fields of view per animal) were obtained in this way. (If the perimeter of the lung section was encountered, the objective was moved two field widths in the positive y direction, and the stepping was continued in the negative x direction.)

The number and length of fibers in each volume were noted by a human operator who was able to move up and down through the depth series of images while looking for the characteristic bright points or lines that indicated a reflective or refractile particle or fiber.

RESULTS

Validation of Lung Digestion Procedure

As described in the earlier publication (Bernstein et al., 2003), comparative confocal microscopy was used to assure that the lung digestion and transmission electron microscopy (TEM) procedures used in this study did not affect the fiber length of the chrysotile present in the lung.

The results of this analysis confirmed that there is a very good correlation between the length distribution as measured by the lung digestion procedure/TEM and the confocal methodology with a correlation $r^2 = .9$ and that the TEM procedure does not reduce the length distribution of the fibers seen in the confocal analysis.

Inhalation Biopersistence

The EC Inhalation Biopersistence Protocol specifies that the exposure atmosphere to which the animals are exposed should have at least 100 fibers/cm³ longer than 20 μm . In this study, the number of fibers longer than 20 μm in the chrysotile exposure atmosphere was purposely increased to a mean of 200 fibers with $L > 20 \mu\text{m}/\text{cm}^3$, in order to maximize any potential effect of these long fibers on clearance from the lung. For tremolite the mean exposure concentration was maintained at 100 fibers with $L > 20 \mu\text{m}/\text{cm}^3$. The number, concentration, and size distribution of the air control, chrysotile, and tremolite exposure groups are shown in Table 1.

The mean number of WHO fibers (defined as fibers $>5 \mu\text{m}$ long, $<3 \mu\text{m}$ wide, and with length:width ratios $>3:1$; WHO, 1997) in the chrysotile exposure atmosphere was 11,053 fibers/cm³, which was more than 100,000 times the OSHA occupational exposure limit for chrysotile of 0.1 fibers/cm³. The tremolite exposure atmosphere had fewer shorter fibers resulting in a mean of 1090 WHO fibers/cm³. The mean total number of fibers of all sizes present in the exposure atmosphere was 48,343 fibers/cm³ for chrysotile and 3128 fibers/cm³ for tremolite.

Details of the length and diameter distribution of the chrysotile and tremolite fibers in the aerosol and in the lung were presented earlier, as were electron micrographs of the collected from the aerosol and as recovered from the lung (Bernstein et al., 2003).

Fiber Clearance

The clearance of fibers from the lung as determined through the lung digestion procedure was examined separately for 3 length ranges of fibers: fibers longer than 20 μm , fibers 5–20 μm in length, and fibers/objects less than 5 μm in length.

Fibers longer than 20 μm in length were used as an index of those fibers that cannot be completely phagocytosed by the macrophage. Because they cannot be effectively cleared from the lung by the macrophage, when fibers in this length range are biopersistent, they have been shown to be associated with fiber-related disease (Bernstein et al., 2001; Hesterberg et al., 1998).

Fibers less than 5 μm in length are effectively not different from nonfibrous particles and are cleared with similar kinetics and mechanism as particles. While longer fibers may also be cleared effectively by the macrophage and as a result not be different in kinetically than particles, the 5- μm cutoff was chosen to mirror the use by the WHO of a 5- μm cutoff in their counting schemes for fibers. As is discussed later, recent reviews of these size fibers have concluded that they present very little or no risk to human health (ATSDR, 2003).

Fibers between 5 and 20 μm in length represent the transition range between those fibers which are cleared as particles and the longer fibers that the macrophage cannot fully phagocytose. The actual limit as to what length fiber can be fully phagocytosed has been proposed for the rat as ranging from 15 μm (Miller, 2000) to 20 μm (Luoto et al., 1995; Morimoto et al., 1994).

The number and size distribution of the fibers recovered from the lungs are summarized in Tables 2 and 3.

The clearance half-times for each of the three length fractions of chrysotile and tremolite are summarized in Table 4.

Figure 3 presents the comparative clearance of Calidria chrysotile and tremolite for fibers with lengths greater than 20 μm . The graph is presented with a log scale for the concentration in order to highlight the relative magnitude in difference that was observed. Even though the number of long fibers in the chrysotile aerosol was nearly twice that of the tremolite aerosol (190.5 chrysotile vs. 106.2 tremolite), by the first sacrifice immediately following the fifth day of exposure, the chrysotile lung burden was already 100 times less that of tremolite. This rapid disintegration/dissolution of the long chrysotile fibers continued with a resulting clearance half-time following the termination of exposure of 7 h. By 2 days postexposure there were no long chrysotile fibers remaining.

In contrast, with tremolite, by the end of the end of the exposure period more than 1.4 million tremolite fibers longer than 20 μm had accumulated in the lung. Following early clearance in the first 24 h, there was no statistically significant ($p < .05$) decrease in tremolite fiber concentration in the lung through 365 days postexposure, as illustrated in Figure 3. Following this short-term clearance, the clearance half-time of the long tremolite fibers was essentially infinite. It should be noted, however, that the coefficients could not be calculated due to the lack of slope.

TABLE 1
Number, concentration, and size distribution of the chrysotile, tremolite, and air control exposure atmosphere

Exposure group	Gravimetric concentration (mg/m ³), mean ± standard deviation	Mean number of fibers evaluated	Mean number of total fibers per cm ³	Mean number of WHO fibers per cm ³	Mean percent of fibers L > 20 μm	Mean number of fibers L > 20 μm of total fibers	Diameter range (μm)	Length range (μm)	GMD (μm) ± standard deviation	GML (μm) ± standard deviation	Mean diameter (μm) ± standard deviation	Mean length (μm) ± standard deviation
Calidria chrysotile	1.69 ± 0.28	2016	48,343.2	11,052.8	22.2	0.4	0.02–0.7	0.07–37.6	0.07 ± 1.94	2.65 ± 3.10	0.08 ± 0.07	3.61 ± 7.37
Tremolite	11.47 ± 1.30	1627	3128.1	1090.3	34.9	3.4	0.1–3.7	0.9–75	0.27 ± 2.06	3.71 ± 3.52	0.32 ± 0.45	5.49 ± 13.97
Air control	0.00	2	0.1	0	0	0	—	—	—	—	—	—

Note.—Not determined.

TABLE 2
Lung burden of Calidria chrysotile—Fiber number and size

Exposure Group	Burden of Calidria chrysotile							
Days after cessation of exposure	0	1	2	7	14	30	90	365
Total number of fibers evaluated	1517	1507	1507	1415	926	657	527	101
Mean number of total fibers per lung lobes ($\times 10^6$)	46.06 \pm 8.21	42.92 \pm 5.82	37.68 \pm 1.53	35.34 \pm 2.24	39.60 \pm 2.00	32.06 \pm 2.74	12.76 \pm 1.11	3.3 \pm 0.6
Mean number WHO fibers per lung lobes ($\times 10^6$)	2.26 \pm 0.55	1.74 \pm 0.13	1.55 \pm 0.10	1.05 \pm 0.15	0.48 \pm 0.01	0.18 \pm 0.06	0.03 \pm 0.01	0.002 \pm 0.005
Mean WHO fibers of total fibers (%)	4.9	4.1	4.1	3.0	1.2	0.5	0.2	0.08
Mean number of fibers L > 20 μm per lung lobes ($\times 10^6$)	0.01 \pm 0.005	0.0	0.0	0.0	0.0	0.0	0.0	0.0
Mean fibers L > 20 μm of total fibers (%)	0.0	0.0	0.0	0.0	0.0	0.0	0.0	0.0
Mean number of fibers L 5–20 μm per lung lobes ($\times 10^6$)	2.25 \pm 0.55	1.74 \pm 0.13	1.55 \pm 0.10	1.05 \pm 0.15	0.48 \pm 0.01	0.18 \pm 0.06	0.03 \pm 0.01	0.002 \pm 0.005
Mean fibers L 5–20 μm of total fibers (%)	4.9	4.1	4.1	3.0	1.2	0.5	0.2	0.08
Diameter range (μm)	0.03–2.5	0.03–1.9	0.03–1.75	0.03–1.8	0.03–1.4	0.03–0.8	0.03–0.53	0.03–0.27
Length range (μm)	0.56–25	0.6–17	0.54–14	0.52–14	0.52–14	0.58–11	0.5–7.84	0.52–5.24
Mean diameter (μm)	0.15	0.16	0.13	0.13	0.09	0.09	0.06	0.06
Standard deviation	0.40	0.35	0.28	0.23	0.19	0.10	0.06	0.04
Mean length (μm)	2.12	2.16	2.03	2.08	1.80	1.63	1.24	1.6
Standard deviation	4.60	4.27	4.01	3.74	3.51	2.58	1.36	0.8
GMD (μm)	0.11	0.12	0.10	0.10	0.08	0.08	0.06	0.06
Standard deviation	3.31	3.12	2.99	2.64	2.48	2.07	1.62	1.57
GML (μm)	1.76	1.81	1.68	1.78	1.56	1.44	1.10	1.4
Standard deviation	3.23	3.14	3.21	2.96	2.85	2.33	1.83	1.6
Length weighted arthm. diameter (μm)	0.21	0.21	0.18	0.16	0.12	0.11	0.07	0.07
Length weighted geom. diameter (μm)	0.15	0.15	0.13	0.12	0.09	0.08	0.06	0.06
Mean aspect ratio mean	19.61	19.22	20.55	21.90	23.91	23.86	22.28	28.06
Mean number of particles evaluated	0.4	0.6	0.0	0.0	0.2	0.2	0.0	0.0
Mean number of particles/lung lobes ($\times 10^6$)	0.00	0.01	0.00	0.00	0.00	0.00	0.00	0.00
$\leq 1 \mu\text{m}$ particles/lung lobes ($\times 10^6$)	0.00	0.00	0.00	0.00	0.00	0.00	0.00	0.00
$> 1 \mu\text{m} - \leq 3 \mu\text{m}$ particles/lung lobes ($\times 10^6$)	0.00	0.00	0.00	0.00	0.00	0.00	0.00	0.00
$> 3 \mu\text{m}$ particles/lung lobes ($\times 10^6$)	0.00	0.00	0.00	0.00	0.00	0.00	0.00	0.00

Figure 4 shows the comparative clearance of the fibers 5–20 μm in length for Calidria chrysotile and tremolite and Figure 5 the comparative clearance of the fibers/objects less than 5 μm in length. Also shown in both graphs is the range of clearance for insoluble nuisance dusts (Muhle et al., 1987a; Stoeber et al.,

1970). The chrysotile fibers 5–20 μm also clear considerably faster than the tremolite fibers. By 365 days, more than 99.9% of the chrysotile 5–20 μm fibers have been eliminated with a clearance half-time of 7 days, with only 4 fibrils measured on the filter from 1 rat out of the 5 examined, with the remaining 4

TABLE 3
Lung burden of tremolite—Fiber number and size

Exposure group	Burden of tremolite							
Days after cessation of exposure	0	1	2	7	14	30	90	365
Total number of fibers evaluated	2022	1876	1923	1848	1868	687	1791	345
Mean number of total fibers per lung lobes ($\times 10^6$)	68.46 \pm 4.72	63.89 \pm 7.05	68.06 \pm 4.70	63.01 \pm 1.98	59.55 \pm 3.41	40.78 \pm 4.35	32.71 \pm 1.72	19.6 \pm 3.2
Mean number WHO fibers per lung lobes ($\times 10^6$)	17.71 \pm 3.36	12.83 \pm 3.67	16.56 \pm 3.49	13.45 \pm 1.24	13.77 \pm 1.38	9.56 \pm 2.76	7.62 \pm 0.53	7.3 \pm 1.9
Mean WHO fibers of total fibers (%)	25.7	19.8	24.2	21.3	23.2	24.9	23.4	37.5
Mean number of fibers L >20 μm per lung lobes ($\times 10^6$)	1.42 \pm 0.26	0.82 \pm 0.30	1.04 \pm 3.37	0.74 \pm 0.12	0.77 \pm 0.04	0.57 \pm 0.20	0.63 \pm 0.08	0.48 \pm 0.13
Mean fibers L > 20 μm of total fibers (%)	2.1	1.3	1.5	1.2	1.3	1.4	1.9	2.5
Mean number of fibers L 5–20 μm per lung lobes ($\times 10^6$)	16.29 \pm 3.15	12.01 \pm 3.41	15.53 \pm 3.15	12.71 \pm 1.27	13.00 \pm 1.37	8.99 \pm 1.89	7.00 \pm 0.48	6.9 \pm 1.8
Mean fibers L 5–20 μm of total fibers (%)	23.7	18.6	22.7	20.1	21.9	21.7	21.5	35.1
Diameter range (μm)	0.056–2.5	0.05–2.2	0.06–2.2	0.044–1.8	0.049–2.1	0.046–2.0	0.032–2.5	0.04–1.9
Length range (μm)	0.7–58	0.65–60	0.7–58	0.62–52	0.54–54	0.51–50	0.54–54	0.58–47.8
Mean diameter (μm)	0.32	0.28	0.32	0.28	0.27	0.25	0.23	0.29
Standard deviation	0.38	0.38	0.35	0.32	0.35	0.33	0.34	0.31
Mean length (μm)	4.46	3.99	4.31	3.83	4.06	4.12	4.47	5.6
Standard deviation	12.40	11.78	12.08	10.44	10.86	10.27	10.78	9.1
GMD (μm)	0.26	0.23	0.27	0.23	0.23	0.21	0.18	0.23
Standard deviation	2.14	2.27	2.09	2.13	2.17	2.18	2.36	2.18
GML (μm)	3.10	2.82	3.04	2.71	2.79	2.73	2.88	3.8
Standard deviation	3.86	3.85	3.77	3.75	3.79	3.66	3.82	3.0
Length weighted arthm. diameter (μm)	0.45	0.41	0.43	0.38	0.38	0.37	0.36	0.23
Length weighted geom. diameter (μm)	0.36	0.33	0.36	0.31	0.31	0.29	0.29	0.20
Mean aspect ratio mean	15.11	15.04	14.77	15.21	15.65	17.05	19.99	20.80
Mean number of particles evaluated	4.0	4.4	4.5	5.2	4.4	4.2	4.2	3.8
Mean number of particles/lung lobes ($\times 10^6$)	0.06	0.05	0.06	0.06	0.05	0.05	0.05	0.04
$\leq 1 \mu\text{m}$ particles/lung lobes ($\times 10^6$)	0.03	0.03	0.02	0.02	0.02	0.02	0.02	0.02
$> 1 \mu\text{m} - \leq 3 \mu\text{m}$ particles/lung lobes ($\times 10^6$)	0.02	0.02	0.03	0.02	0.02	0.03	0.02	0.02
$> 3 \mu\text{m}$ particles/lung lobes ($\times 10^6$)	0.01	0.00	0.00	0.01	0.01	0.01	0.00	0.00

rats having 0 fibers. This extrapolates to 2000 fibrils per lung in 1 out of the 5 lungs examined. In the tremolite-exposed animals, following short-term clearance during the first 30 days, there is little further clearance with nearly 7 million fibers per lung 5–20 μm in length remaining in the lung at 365 days.

The short fibers/objects less than 5 μm in length are used as index of those fibers which can be cleared with similar kinetics and pathways as non-fibrous particles. The clearance of short

fiber Calidria chrysotile is seen in Figure 5 to fall within the range of clearance of insoluble nuisance dusts. This clearance is faster than that of the short fiber tremolite. Two factors may influence these results. First, numerous biopersistence studies on synthetic vitreous fibers have shown that while the dissolution kinetics are generally slower in the pathways taken by the shorter fibers, dissolution still does occur for these length fibers. Thus, the chrysotile may continue to break apart while the tremolite

TABLE 4
Clearance half-times of Canadian chrysotile and tremolite by length fraction

Fiber length	Calidria chrysotile	Tremolite
>20 μm	$T_{1/2} = 0.31 \text{ days}^a$	$WT_{1/2} = \infty \text{ days}^{b,c}$
5–20 μm	$T_{1/2} = 7.0 \text{ days}^a$	$WT_{1/2} = \infty \text{ days}^{b,c}$
<5 μm	$T_{1/2} = 64.0 \text{ days}^a$	$WT_{1/2} = 151.5 \text{ days}^{b,c}$

Note. All data were fit using statistical methods as recommended in the European Commission guidelines (Bernstein & Riego-Sintes, 1999).

^aData best fit to a single exponential.

^bData best fit to a double exponential.

^cWeighted half-time was greater than 50,000 days.

would not. Second, during the inflammatory cellular response induced by the longer fiber tremolite, any shorter fibers either in the macrophages or nearby may be trapped by the cells and eventually be included in granulomas. These trapped shorter fibers will no longer have the same clearance kinetics as before; however, when the lung is digested these shorter fibers will be released and included with the other short fibers in the counting statistics.

Lung Weights

The weight of the lungs at necropsy can be influenced by inflammatory response to a material following inhalation. Table 5

presents the mean (\pm standard deviation) lung weights in the air control group, the chrysotile-exposed group, and the tremolite-exposed group at each sacrifice time point after cessation of the 5-day exposure period. Also shown in the last column are those groups for which there were statistically significant differences in the means. At no time point were there any significant differences in mean values between the air controls and the chrysotile exposure group. At all time points at which the air control group was evaluated, the mean tremolite group lung weights were significantly greater than the air control, and through 90 days they were significantly greater than the chrysotile group.

Histopathology

While the fiber clearance results sharply differentiate Calidria chrysotile fiber retention from that of tremolite, the histopathology findings provide a pathological basis for evaluating the importance of this difference.

The summary incidence of the histopathological findings in the lung at days 1, 2, 14, and 90, 180, and 365 days after cessation of exposure are presented in the Appendix in Tables A1 through A6. Shown are the specific histological findings seen in the lung, the number of animals per dose group examined, and the number of animals with each grade of the finding. For each finding the total number of animals affected and the mean severity are also shown.

There were no exposure-related histopathological findings in the rats exposed to either filtered air (air control) or in the rats exposed to Calidria chrysotile. There was no indication of any

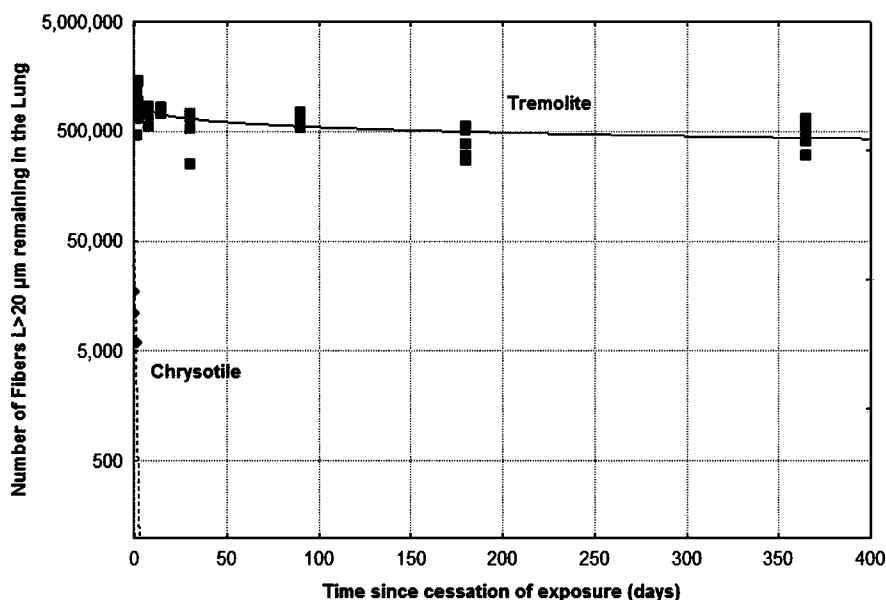


FIG. 3. Clearance of Calidria chrysotile and tremolite fibers with length $>20 \mu\text{m}$. Graph showing the clearance of the Calidria chrysotile and tremolite fibers longer than $20 \mu\text{m}$ from the lung following cessation of the 5-day exposure period. The diamonds indicate the number of chrysotile fibers remaining in the individual lungs and the squares the number of tremolite fibers remaining. The lines are the clearance curves for each fitted to the data using non-linear regression techniques with a single exponential (StatSoft, Inc., 2003) as specified by the EC Guidelines (Bernstein & Riego-Sintes, 1999). The clearance half-times are presented in Table 4.

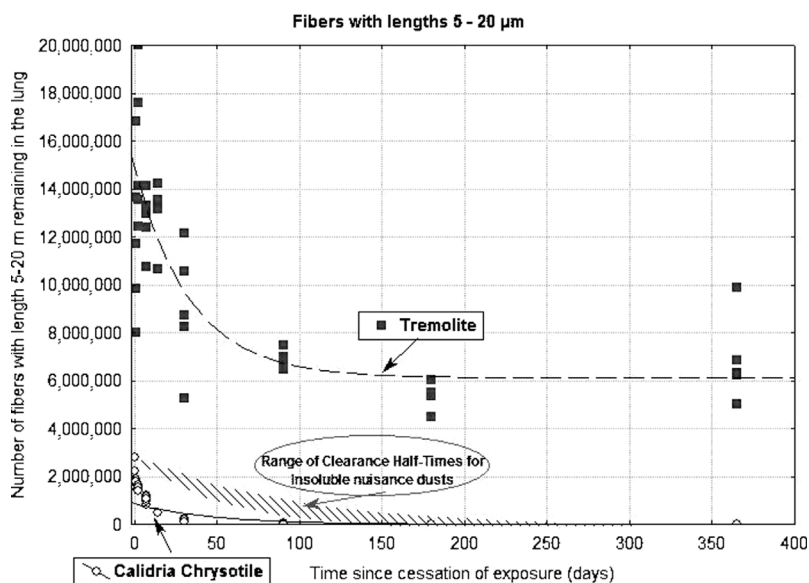


FIG. 4. Clearance of Calidria chrysotile and tremolite fibers with length 5–20 μm . Graph showing the clearance of the Calidria chrysotile and tremolite fibers 5–20 μm in length from the lung following cessation of the 5-day exposure period. The circles indicate the number of chrysotile fibers remaining in the individual lungs and the squares the number of tremolite fibers remaining. The lines are the clearance curves for each fitted to the data using non-linear regression techniques with a single exponential (StatSoft, Inc., 2003) as specified by the EC Guidelines (Bernstein & Riego-Sintes, 1999). Also shown in is the range of clearance for insoluble nuisance dusts (Muhle et al., 1987; Stoeber et al., 1970).

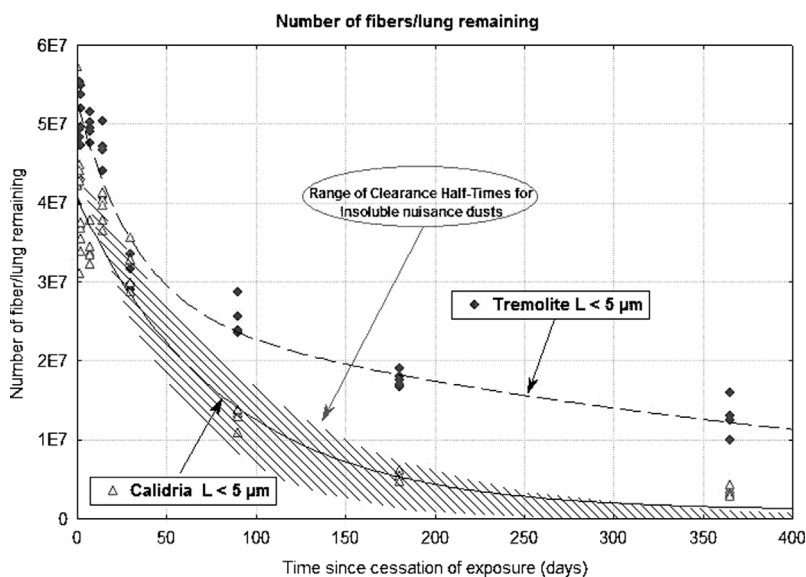


FIG. 5. Clearance of Calidria and tremolite $L > 5 \mu\text{m}$. Graph showing the clearance of the Calidria chrysotile and tremolite fibers shorter than 5 μm in length from the lung following cessation of the 5-day exposure period. The circles indicate the number of chrysotile fibers remaining in the individual lungs and the squares the number of tremolite fibers remaining. The lines are the clearance curves for each fitted to the data using nonlinear regression techniques with a single exponential (StatSoft, Inc., 2003) as specified by the EC Guidelines (Bernstein & Riego-Sintes, 1999). Also shown in is the range of clearance for insoluble nuisance dusts (Muhle et al., 1987; Stoeber et al., 1970).

TABLE 5
Lung weights in grams: mean \pm standard deviation ($n = 7$)

Time postexposure (days)	Group 1, air control	Group 2, calidria chrysotile	Group 3, tremolite	Statistically significant mean differences ^a
1	1.062 \pm 0.083	1.073 \pm 0.059	1.241 \pm 0.117	Air-Trem $p = .006$ Calidia-Trem $p = .005$
2	N.W.	0.971 \pm 0.078	1.202 \pm 0.139	Calidia-Trem $p = .002$
7	N.W.	1.066 \pm 0.056	1.237 \pm 0.056	Calidia-Trem $p = 0.001$
14	N.W.	1.138 \pm 0.085	1.250 \pm 0.086	Calidia-Trem $p = .031$
30	1.144 \pm 0.103	1.179 \pm 0.049	1.340 \pm 0.150	Air-Trem $p = 0.014$ Calidia-Trem $p = .019$
90	N.W.	1.233 \pm 0.159	1.381 \pm 0.077	Calidia-Trem $p = .047$
180	1.325 \pm 0.106	1.396 \pm 0.101	1.526 \pm 0.137	Air-Trem $p = .025$
365	1.417 \pm 0.041	1.459 \pm 0.14	1.518 \pm 0.089	Air-Trem $p = .043$

Note. N.W., The control group was not sacrificed/weighed at these time points. Trem, tremolite.

^aDunnett test based on pooled variance.

inflammatory response in the lung at any time point following the Calidria chrysotile exposure.

In contrast, rats exposed to tremolite showed an immediate inflammatory response at the sacrifice following termination of the last exposure. The cellular lesions observed were characterized by alveolar macrophage aggregation and microgranulomas. In the rats sacrificed after the 1- and 2-day observation periods, alveolar lining cell hypertrophy/hyperplasia, and bronchiolitis were noted. At both 14 days and 90 days after cessation of exposure, fibrosis characterized by collagen deposition was diagnosed in microgranulomas in addition to the cellular lesions. At 90 days after cessation of exposure, the fibrosis in the granulomas has increased in severity up to grade 2.8 and interstitial fibrosis is seen already in 1 animal and per-

sisted through 180 days. At 12 mo postexposure, granulomas at the bronchoalveolar junction were noted with some fibrosis in the granulomas. Moderate erythrophagocytosis was noted in the mediastinal lymph node of 1 rat. No pleural lesions were noted.

Photomicrographs of the tremolite, chrysotile, and filtered-air (control) exposed lungs are shown in Figures 6 through 11. Additional photomicrographs of the earlier time points were presented in Bernstein et al. (2003b). As seen in Figure 6, the granulomas, which are composed initially of aggregates of macrophages and/or epithelioid cells, are already well formed at 1 day after cessation of the 5-day exposure. By 90 days (Figure 7), fibrosis is seen in the granulomas. In addition, interstitial fibrosis is also observed. As shown in Figures 8 and 9,

TABLE 6
Mean degree of cellular lesions^a and fibrosis at the different sacrifice time points in rats exposed to tremolite^b

Time (days) after cessation of exposure	Figure	Alveolar macrophage	Granuloma	Fibrosis granuloma	Interstitial fibrosis
1 day	10	2.4	2.6	0	0
2 days		3.0	3.0	0	0
14 days		2.6	3.0	1.0	0
90 days	11	0.5	2.8	2.8	0.5
180 days		2.0	2.5	1.8	0.5
365 days	12	0	0.8	1.0	0

^aThe severity of histologic changes was scored minimal, slight, moderate, marked, and massive (grades 1–5, respectively) A score of zero indicates that this finding was not observed.

^bThe tables presenting the degree of cellular lesions and fibrosis results in the initial publication (Bernstein et al., 2003) presented the means of only animals with a nonzero positive response as initially reported by the pathologist. This was not considered to be a true indicator of the group mean. This has been corrected with the mean values in Table 6 and Tables A1–A6 showing the group mean of all animals including those with no response (zero).

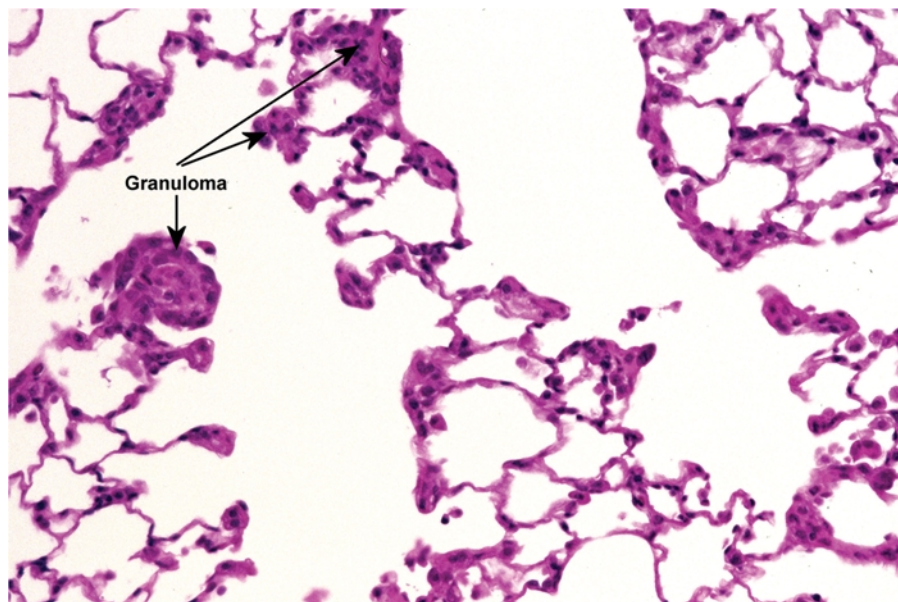


FIG. 6. Histopathology tremolite at 1 day after cessation of exposure. Photomicrograph of a histopathological section from a tremolite-exposed lung 1 day following cessation of the 5-day exposure showing the well-developed granulomatous response.

by 1 year postexposure, granulomas with fibrosis are still present in the lung although with decreased incidence.

In comparison, Figures 10 and 11 show a Calidria chrysotile-exposed lung and the filtered-air control lung, respectively, which are remarkably similar with no inflammatory response observed in either group.

DISCUSSION

The results of this study clearly differentiate Calidria chrysotile from the amphibole tremolite. Calidria chrysotile rapidly clears/disintegrates from the lung, with the long fibers clearing with a half-time of 7 h, faster than any commercial fiber type. By 1 day postexposure there were no fibers remaining

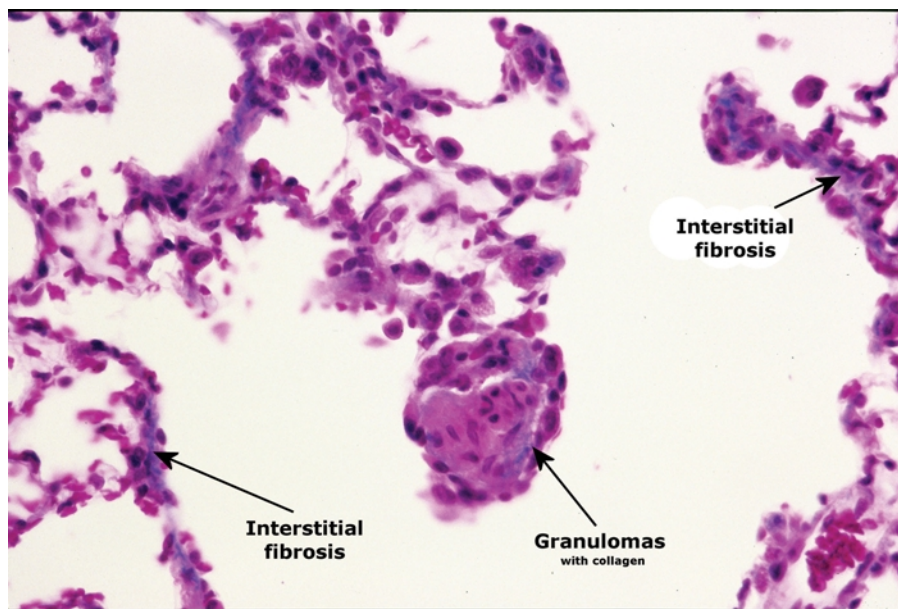


FIG. 7. Histopathology tremolite at 90 days after cessation of exposure. Photomicrograph of a histopathological section from a tremolite-exposed lung 90 days following cessation of the 5-day exposure. The severity of the fibrosis in the granulomas has increased, and the granuloma can be seen interlaced with collagen. By this time the collagen has progressed into the interstitium and interstitial fibrosis is seen as well. Numerous macrophage aggregates are also observed, as well as multinucleated giant cells.

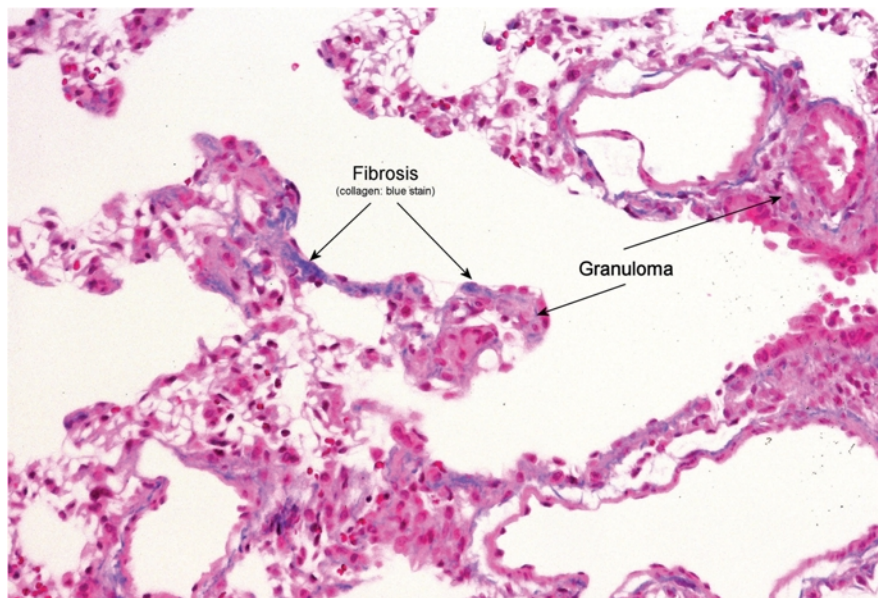


FIG. 8. Histopathology tremolite at 1 yr postexposure, $\times 250$ Trichrome. Photomicrograph of a histopathological section from a tremolite-exposed lung 1 yr following cessation of the 5-day exposure. Granulomas with fibrosis are still present in the lung although with decreased incidence.

longer than $20\ \mu\text{m}$. Even the fibers $5\text{--}10\ \mu\text{m}$ in length clear very rapidly with a half-time of 7 days, again faster than most other commercial fibers.

This is in marked contrast with tremolite, which is essentially insoluble and does not appear to break apart in the lung. The long fibers once deposited remain over the rat's lifetime and even the shorter fibers, following early clearance, also remain with no

dissolution or further removal. At 365 days postexposure, there was a mean lung burden was of 0.5 million fibers $L > 20\ \mu\text{m}$ and 7 million fibers $5\text{--}20\ \mu\text{m}$ in length with a total lung burden of 19.6 million fibers.

This contrast is reinforced with the results of the histopathological examination. Calidria chrysotile, even with exposure to more than $48,000$ total fibers/ cm^3 , did not produce any

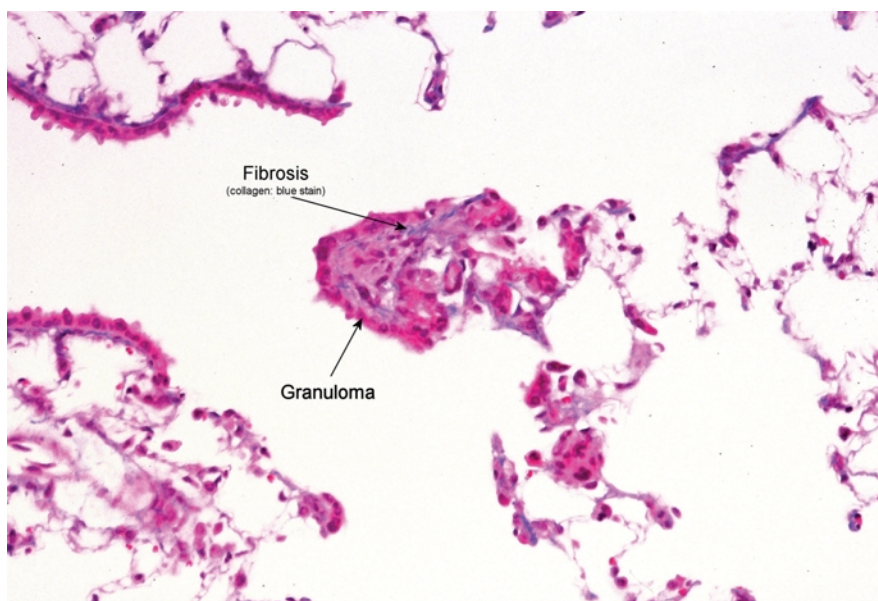


FIG. 9. Histopathology tremolite at 1 yr postexposure, $\times 400$ trichrome. Photomicrograph of a histopathological section from a tremolite-exposed lung 1 yr following cessation of the 5-day exposure. Granulomas with fibrosis are still present in the lung although with decreased incidence.

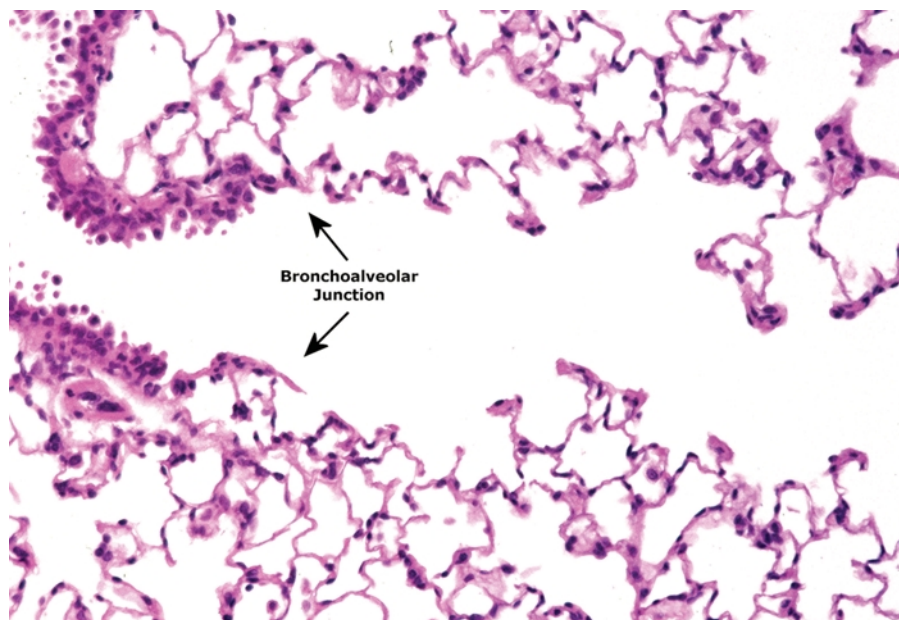


FIG. 10. Histopathology Calidria chrysotile at 2 days postexposure. Photomicrograph of a histopathological section from a Calidria chrysotile exposed lung 2 days following cessation of the 5-day exposure. A few macrophages are seen, which is not surprising considering the recent 5 days of exposure to an atmosphere of more than 48,000 fibers/cm³. Overall, the lungs of the chrysotile-exposed animals were remarkable similar to the lungs of animals from the air control group that received filtered air, an example of which is shown in Figure 11.

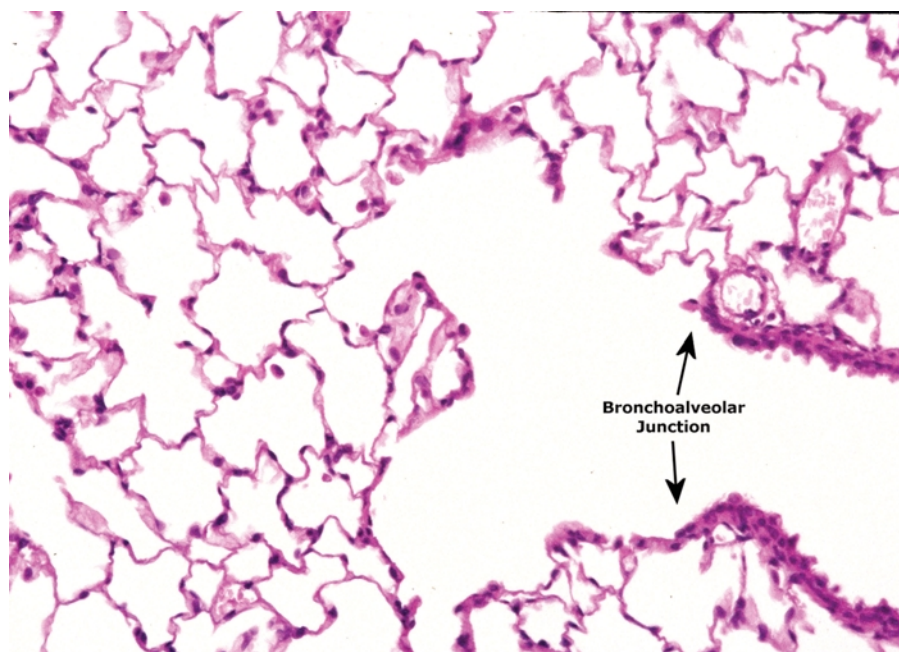


FIG. 11. Histopathology filtered-air control chrysotile at 1 day postexposure. Photomicrograph of a histopathological section from a filtered air control lung 1 day following cessation of the 5-day filtered air exposure.

inflammatory response and the lungs of the chrysotile exposed rats could not be distinguished from those rats that breathed filtered air. The mean lung weights at all time points measured were not statistically different from the air controls.

The tremolite-exposed rats, even with exposure to 16 times fewer total fibers, showed a pronounced inflammatory response to this 5-day exposure with the rapid development of granulomas as seen at day 1 postexposure, followed by the development of collagen deposition within these granulomas and by 90 days even mild interstitial fibrosis.

Influence of Mineralogical Structure of Chrysotile and Tremolite on Biopersistence

Both of these fibers are known as asbestos; however, their mineral structure makes them different and explains why one can be rapidly removed from the lung without inflammation and the other cannot.

Chrysotile is a sheet silicate, while tremolite and other amphiboles are double-chain silicates. As described earlier, the cleavage points in the amphiboles, such as tremolite, result in the mineral splitting into fibers that remain highly insoluble thereafter. The cations in the remaining fiber are bonded by covalent bonds, which are very strong and remain impervious to attack in the lung.

The formation of the fibrous shape with the serpentine, chrysotile, is very different from that of the amphiboles. With chrysotile, the mineral is physically a very thin sheet. Because of the mismatch in the spacing between the magnesium and silica ions, the thin sheet curls, forming a fiber shape as would a rolled sheet of paper. The individual layers of this sheet are 7 Å thick and attached to each other by weak van der Waals bonds (Klein & Hurlbut, 1985). Even the Si—O bond has ~50% covalent character (Liebau, 1985, pp. 46–48). This thin sheet is more fragile and can break, the brucite (Mg^{2+}) layer can dissolve in water or the lung fluid, and the remaining structure can be attacked in an acid environment such as is encountered with the macrophage. Thus with the weak van der Waals bonds, deterioration of the chrysotile surface can result in the loss of the structural integrity of the fiber and the subsequent falling apart into small pieces. Even a small amount of instability may result in the fiber breaking apart.

With tremolite, as described earlier, the potential breakages run along the silica chains. The chains themselves don't break as easily because the bonds between the silica tetrahedra are very strong compared to the weak bonds gluing one chain to the next. Thus when tremolite breaks it splits into fibers that subsequently are very stable.

Factors in the Formation of the Calidria Chrysotile and Their Influence on Biopersistence

In the New Idria body from which Calidria chrysotile was mined, the serpentine was formed from the parent olivine-rich assemblage far beneath the surface (Coleman, 1957). The subsequent tectonic forces pushed the resultant serpentinite mass into

the overlying sedimentary rocks. The total thickness of the serpentinite and of the asbestos ore is not known; however, Byerly (1954, p. 48) has estimated that the body extends to a depth of 15,000 ft (~500 m).

During and after emplacement the ore body was extensively sheared and competent blocks of serpentinite were broken and crushed against one another, much as a thick paste is smeared out and pulverized in a wet ball mill or in a mix-muller. The end product today is a highly friable, soft asbestos ore, containing variable amounts of uncrushed, residual serpentinite rock.

In addition, the shearing that this body has experienced permitted groundwaters to move freely through the rock. Much of the brucite produced during the initial serpentinization probably dissolved in these waters and precipitated later as either hydromagnesite in the surface weathering zone, or as massive deposits of magnesite such as that found in the northwest corner of the serpentinite (Mumpton & Thompson, 1975).

This pulverization and dissolution resulted in the Calidria chrysotile being of very short fiber length. The pulverization and dissolution that occurred naturally appears to have facilitated the ability of the lung to further break apart the chrysotile and effectively clear it as a particle with a clearance half-time of the long fibers of 7 h. As noted, even the clearance of the shorter fibers less than 5 μm in length is faster than that reported for insoluble nuisance dusts.

The importance of these remaining shorter fibers has been addressed in a recent report issued by the Agency for Toxic Substances and Disease Registry entitled "Expert Panel on Health Effects of Asbestos and Synthetic Vitreous Fibers: The Influence of Fiber Length." The panel stated that "Given findings from epidemiologic studies, laboratory animal studies, and in vitro genotoxicity studies, combined with the lung's ability to clear short fibers, the panelists agreed that there is a strong weight of evidence that asbestos and SVFs (synthetic vitreous fibers) shorter than 5 μm are unlikely to cause cancer in humans" (ATSDR, 2003; U.S. EPA, 2003). Berman and Crump (2003) in their technical support document to the U.S. EPA on asbestos-related risk also found that shorter fibers do not appear to contribute to carcinogenic risk.

It is interesting to note that in short term exposure (3 days) of rodents to urban particulate matter at mass exposure concentrations an order of magnitude lower than in our study, a significant inflammatory response was noted (Clarke et al., 1999).

Comparison with Other Fibers

To date, the inhalation biopersistence of three different chrysotile asbestos have been evaluated. These include Canadian chrysotile (Bernstein et al., 2005), Brazilian chrysotile (Bernstein et al., 2004), and this study on Calidria chrysotile. In all of these studies, chrysotile was found to clear rapidly from the lung with clearance half-times of the fiber longer than 20 μm ranging from 0.3 days for Calidria, 1.3 days for the Brazilian chrysotile, and 11.4 days for the Canadian chrysotile. In the Canadian study, a textile grade of chrysotile was chosen

which was specifically produced to have thin long fibers of the type used in the production of textiles.

In the Canadian and Brazilian studies, confocal microscopy was used to determine translocation and distribution of chrysotile fibers within the lung. The large majority of fibers was found in the parenchyma, with most of those found in the alveolar macrophages. Again this reinforces the importance of the acid milieu of the macrophage in mediating the dissolution and breakage of the chrysotile. While these studies did not include standard histopathological examination, inflammatory cells were identified by examination in serial section image data of the nuclear morphology of the cells and the surrounding pulmonary tissue with mononuclear cells, such as alveolar macrophages, easily distinguished from neutrophils, which exhibit polymorphonuclear profiles. In both of these studies neutrophils were not observed free in alveolar spaces or in any of the data volumes collected. Neutrophil-mediated inflammatory re-

sponse did not occur in the presence of chrysotile fibers at any of the time points examined. In addition, many of the shorter fibers that remained were observed in the alveoli where they no longer attracted macrophages. These fibers appeared to be coated by the lung, neutralizing cellular response. (Bernstein et al., 2004, 2005).

As the serpentine asbestos, chrysotile, is a naturally occurring mined fiber, there appear to be small differences in biopersistence depending on the commercial grade tested. Table 7 summarizes the range of clearance half-times reported in inhalation biopersistence studies on mineral fibers. Chrysotile lies on the soluble end of this scale and ranges from Calidria chrysotile, the least biopersistent fiber, to a fiber with biopersistence in the range of glass and stone wools. It remains less biopersistent than ceramic and special-purpose glasses (Hesterberg et al., 1998) and as seen in the current study more than 100 times less biopersistent than the amphibole asbestos.

TABLE 7

Comparative clearance half-times of fibers longer than 20 μm and fibers between 5 and 20 μm for chrysotile, synthetic vitreous fibers, and amphiboles

Fiber	Type	Clearance Half-time ($T_{1/2}$) (days)		Reference
		Fibers length >20 μm	Fibers length 5–20 μm	
Calidria chrysotile	Serpentine asbestos	0.3	7	Current study
Brazilian chrysotile	Serpentine asbestos	1.3	2.4	Bernstein et al., 2004
Fiber B (B01.9)	Experimental glass wool	2.4	11	Bernstein et al., 1996
Fiber A	Glass wool	3.5	16	Bernstein et al., 1996
Fiber C	Glass wool	4.1	15	Bernstein et al., 1996
Fiber G	Stone wool	5.4	23	Bernstein et al., 1996
MMVF34 (HT)	Stone wool	6	25 ^a	Hesterberg et al., 1998
MMVF22	Slag wool	8.1	77	Bernstein et al., 1996
Fiber F	Stone wool	8.5	28	Bernstein et al., 1996
MMVF11	Glass wool	8.7	42	Bernstein et al., 1996
Fiber J (X607)	Calcium, magnesium, silicate	9.8	24	Bernstein et al., 1996
Canadian chrysotile (Textile grade)	Serpentine asbestos	11.4	29.7	Bernstein et al., 2005
MMVF 11	Glass wool	13	32	Bernstein et al., 1996
Fiber H	Stone wool	13	27	Bernstein et al., 1996
MMVF10	Glass wool	39	80	Bernstein et al., 1996
Fiber L	Stone wool	45	57	Bernstein et al., 1996
MMVF21	Stone wool	46	99	Bernstein et al., 1996
MMVF33	Special-purpose glass	49	72 ^a	Hesterberg et al., 1998
RCF1a	Refractory ceramic	55	59 ^a	Hesterberg et al., 1998
MMVF21	Stone wool	67	70 ^a	Hesterberg et al., 1998
MMVF32	Special-purpose glass	79	59 ^a	Hesterberg et al., 1998
Amosite	Amphibole asbestos	418	900 ^a	Hesterberg et al., 1998
Crocidolite	Amphibole asbestos	536	262	Bernstein et al., 1996
Tremolite	Amphibole asbestos	—	—	Current study

^aThe $T_{1/2}$ for fibers 5–20 μm in length was not reported by Hesterberg et al. (1998); the values shown were calculated from the raw data by D. Bernstein.

Many publications have reported on toxic effects of chrysotile in *in vitro* studies. However, these studies are difficult to interpret as the *in vitro* systems used are usually not dynamic and as a result can not take into account the dissolution of the fiber as it occurs *in vivo*. In addition, these *in vitro* studies use very high concentrations of fibers in order to produce an effect, often many orders of magnitude higher than occurs during human exposure. Donaldson and Tran (2004), in a recent review on the use of short-term studies in evaluating respirable industrial fibers, stated that short-term biological tests are likely to produce false positives in the case of long, nonbiopersistent fibers, because while they may have effects *in vitro*, they do not persist long enough in the lungs for sufficient dose to build up and produce effects *in vivo*.

As discussed in detail in the earlier publication (Bernstein et al., 2003), Ilgren and Chatfield (1997, 1998a, 1998b) and Muhle et al. (1987a) reported that following chronic inhalation toxicology studies with Calidria chrysotile that no fibrotic or tumorigenic response was observed. In contrast, Davis et al. (1985) reported that following chronic inhalation exposure to tremolite fiber, which, was similar to that used in the current study, "tremolite thus proved to be the most dangerous mineral that we have studied."

Chronic inhalation studies of chrysotiles from other locations, however, have not shown the same differentiation. Berman et al. (1995) stated that this may be due at least in part to the limited lifetime of the rat relative to the biodegradability of the asbestos fiber types evaluated in these studies. However, it should be noted as well that at the mass dose of 10 mg/m³ used in most chrysotile chronic inhalation studies, the corresponding exposure concentration was approximately 1,000,000 particles and fibers/cm³, 90% of which were particles or short fibers. High concentrations of insoluble nuisance dusts have been shown to compromise the clearance mechanisms of the lung, causing inflammation and a tumorigenic response in the rat, a phenomenon often referred to as lung overload (Bolton et al., 1983; Muhle et al., 1987b; Morrow, 1988; Oberdorster, 1995; Bellmann et al., 2003).

Recent quantitative reviews of epidemiological studies of mineral fibers have determined the potency of chrysotile and amphibole asbestos for causing lung cancer and mesothelioma in relation to fiber type also differentiated between these two minerals (Hodgson & Darnton, 2000; Berman & Crump, 2003). The most recent analyses also concluded that it is the longer, thinner fibers that have the greatest potency. However, these studies did not differentiate exposure by source and as a result the unique case of Calidria chrysotile was not specifically addressed in these epidemiological studies.

CONCLUSIONS

The curled mineralogical structure of the sheet silica chrysotile results in a dramatically different behavior in the lung

in comparison to the amphibole double-chain silicas such as tremolite. The tectonic forces active in the formation of the Calidria chrysotile ore deposit have resulted in the formation of an even more unique fiber as the serpentine mass was broken and crushed and then dissolved through filtration of the groundwater. This pulverization and dissolution resulted in the Calidria chrysotile being of very short fiber length.

Following the 5-day exposure to 190 fibers/cm³ longer than 20 μm (total fiber exposure of 48,000 fibers/cm³), the Calidria chrysotile cleared from the lung with a half-time of 0.3 days, 7 hours, which is faster than any other commercial mineral fiber. The fibers 5–20 μm also cleared rapidly with a half time of 7 days. Even the clearance of the shorter fibers less than 5 μm in length is faster than that reported for insoluble nuisance dusts. This exposure to chrysotile did not produce any inflammatory response, and the lungs of the chrysotile exposed rats could not be distinguished from those rats that breathed filtered air.

This is in marked contrast to the exposure to tremolite, which is essentially insoluble and does not appear to break apart in the lung. The long fibers once deposited remain over the rat's lifetime with essentially an infinite half-time and even the shorter fibers, following early clearance, also remain with no dissolution or further removal. At 365 days postexposure, there was a mean lung burden was of 0.5 million fibers L > 20 μm and 7 million fibers 5–20 μm in length with a total lung burden of 19.6 million fibers. The tremolite exposed rats, even with exposure to 16 times fewer total fibers than chrysotile, showed a pronounced inflammatory response with the rapid development of granulomas as seen at day 1 postexposure, followed by the development of fibrosis within these granulomas and by 90 days even mild interstitial fibrosis.

These findings provide an important basis for substantiating both kinetically and pathologically the differences between chrysotile and the amphibole tremolite. This has been demonstrated for three different chrysotile samples from Canada, the United States, and Brazil. As Calidria chrysotile has been certified to have no tremolite fiber, the results of the current study together with the results from toxicological and epidemiological studies indicate that this fiber is not associated with lung disease.

REFERENCES

- Agency for Toxic Substances and Disease Registry. 2003. *Report on the Expert Panel on Health Effects of Asbestos and Synthetic Vitreous Fibers: The influence of fiber length*. Atlanta, GA: Prepared for Agency for Toxic Substances and Disease Registry Division of Health Assessment and Consultation.
- Badollet, M. S. 1948. Research on asbestos fibers. *Can. Min. Metal Trans.* 51:48–51.
- Badollet, M. S. 1951. Asbestos a mineral of Unparalleled properties. *Trans. Can. Inst. Mining Met.* 54:152.
- Bellmann, B., Muhle, H., Creutzenberg, O., Ernst, H., Muller, M., Bernstein, D. M., and Riego Sintes, J. M. 2003. Calibration study

- on subchronic inhalation toxicity of man-made vitreous fibers in rats. *Inhal. Toxicol.* 15(12):1147–1177.
- Berman, D. W., and Crump, K. S. 2003. *Technical support document for a protocol to assess asbestos-related risk*. Washington, DC: Office of Solid Waste and Emergency Response, U.S. Environmental Protection Agency.
- Berman, D. W., Crump, K. S., Chatfield, E. J., Davis, J. M., and Jones, A. D. 1995. The sizes, shapes, and mineralogy of asbestos structures that induce lung tumors of mesothelioma in AF/HAN rats following inhalation. *Risk Anal.* 15(2):181–195.
- Bernstein, D. M., and Riego-Sintes, J. M. R. 1999. *Methods for the determination of the hazardous properties for human health of man made mineral fibers (MMMMF)*. Vol. EUR 18748 EN, April. 93, <http://ecb.ei.jrc.it/DOCUMENTS/Testing-Methods/mmmfweb.pdf>. European Commission Joint Research Centre, Institute for Health and Consumer Protection, Unit: Toxicology and Chemical Substances, European Chemicals Bureau.
- Bernstein, D. M., Chevalier, J., and Smith, P. 2003. Comparison of Calidria chrysotile asbestos to pure tremolite: Inhalation biopersistence and histopathology following short-term exposure. *Inhal. Toxicol.* 15(14):1387–1419.
- Bernstein, D. M., Mast R., Anderson, R., Hesterberg, T. W., Musselman, R., Kamstrup, O., and Hadley, J. 1994. An experimental approach to the evaluation of the biopersistence of respirable synthetic fibers and minerals. *Environ. Health Perspect.* 102(suppl 5):15–18.
- Bernstein, D. M., Morscheidt, C., Grimm, H.-G., Thévenaz, P., and Teichert, U. 1996. Evaluation of soluble fibers using the inhalation biopersistence model, a nine-fiber comparison. *Inhal. Toxicol.* 8(4):345–385.
- Bernstein, D. M., Riego Sintes, J. M., Ersboell, B. K., and Kunert, J. 2001. Biopersistence of synthetic mineral fibers as a predictor of chronic inhalation toxicity in rats. *Inhal. Toxicol.* 13(10):823–849.
- Bernstein, D. M., Rogers, R., and Smith, P. 2004. The biopersistence of Brazilian chrysotile asbestos following inhalation. *Inhal. Toxicol.* 16(9):745–761.
- Bernstein, D. M., Rogers, R., and Smith, P. 2005. The biopersistence of Canadian chrysotile asbestos following inhalation: Final results through 1 year after cessation of exposure. *Inhal. Toxicol.* 17(1):1–14.
- Bolton, R. E., Vincent, J. H., Jones, A. D., Addison, J., and Beckett, S. T. 1983. An overload hypothesis for pulmonary clearance of UICC amosite fibres inhaled by rats. *Br. J. Ind. Med.* 40:264–272.
- Byerly, P. E. 1954. *Regional gravity in the central Coast Ranges and the San Joaquin Valley, California*. PhD thesis (cited in Mumpton and Thompson, 1975), Harvard University, Cambridge, MA.
- Cannon, W. C., Blanton, E. F., and McDonald, K. E. 1983. The flow-past chamber: An improved nose-only exposure system for rodents. *Am. Ind. Hyg. Assoc. J.* 44(12):923–928.
- Clarke, R. W., Catalano, P. J., Koutrakis, P., Murthy, G. G., Sioutas, C., Paulauskis, J., Coull, B., Ferguson, S., and Godleski, J. J. 1999. Urban air particulate inhalation alters pulmonary function and induces pulmonary inflammation in a rodent model of chronic bronchitis. *Inhal. Toxicol.* 11(8):637–656.
- Coleman, R. G. 1957. *Mineralogy and petrology of the New Idria District, California*. PhD Thesis (cited in Mumpton and Thompson, 1975), Stanford University, Stanford, CA.
- Coleman, R. G. 1996. New Idria serpentinite: A land management dilemma. *Environ. Eng. Geosci.* II(1):9–22.
- Davis, J. M., Addison, J., Bolton, R. E., Donaldson, K., Jones, A. D., and Miller, B. G. 1985. Inhalation studies on the effects of tremolite and brucite dust in rats. *Carcinogenesis* 6(5):667–674.
- Donaldson, K., and Tran, C. L. 2004. An introduction to the short-term toxicology of respirable industrial fibers. *Mutat. Res.* 553(1–2): 5–9.
- Hargreaves, A., and Taylor, W. H. 1946. An x-ray examination of decomposition products of chrysotile (asbestos) and serpentine. *Miner. Mag.* 27:204–216.
- Hesterberg, T. W., Chase, G., Axten, C., Miller, W. C., Musselman, R. P., Kamstrup, O., Hadley, J., Morscheidt, C., Bernstein, D. M., and Thevenaz, P. 1998. Biopersistence of synthetic vitreous fibers and amosite asbestos in the rat lung following inhalation. *Toxicol. Appl. Pharmacol.* 151(2):262–275.
- Hodgson, A. A. 1979. Chemistry and physics of asbestos. In *Asbestos: properties, applications and hazards*, eds. L. M. Chissick and S. S. Chissick, pp. New York: John Wiley & Sons. pp. 67–114.
- Hodgson, J. T., and Darnton, A. 2000. The quantitative risks of mesothelioma and lung cancer in relation to asbestos exposure. *Ann. Occup. Hyg.* 44(8):565–601.
- Ilgren, E., and Chatfield, E. 1997. Coalinga fiber—A short, amphibole-free chrysotile. Evidence for lack of fibrogenic activity. *Indoor Built Environ.* 6:264–276.
- Ilgren, E., and Chatfield, E. 1998a. Coalinga fiber—A short, amphibole-free chrysotile. Part 2: Evidence for lack of tumorigenic activity. *Indoor Built Environ.* 7:18–31.
- Ilgren, E., and Chatfield, E. 1998b. Coalinga fiber: A short, amphibole-free chrysotile, Part 3: Lack of biopersistence. *Indoor Built Environ.* 7:98–109.
- Ilgren, E., and Chatfield, E. 2002. Coalinga fiber—A short, amphibole-free chrysotile, Part 4: Further evidence for a lack of fibrogenic and tumorigenic activity. *Indoor Built Environ.* 11:171–177.
- Klein, C., and Hurlbut, C. S., Jr. 1985. *Manual of mineralogy*, ed. J. D. Dana, 20th ed. New York: Wiley.
- Liebau, F. 1985. *Structural chemistry of silicates*. Berlin: Springer Verlag.
- Luoto, K., Holopainen, M., Kangas, J., Kalliokoski, P., and Savolainen, K. 1995. The effect of fiber length on the dissolution by macrophages of rockwool and glasswool fibers. *Environ. Res.* 70(1):51–61.
- Miller, F. J. 2000. Dosimetry of particles: Critical factors having risk assessment implications. *Inhal. Toxicol.* 12(suppl. 3):389–395.
- Morimoto, Y., Yamato, H., Kido, M., Tanaka, I., Higashi, T., Fujino, A., and Yokosaki, Y. 1994. Effects of inhaled ceramic fibers on macrophage function of rat lungs. *Occup. Environ. Med.* 51(1): 62–67.
- Morrow, P. E. 1988. Possible mechanisms to explain dust overloading of the lungs. *Fundam. Appl. Toxicol.* 10(3):369–384.
- Muhle, H., Pott, F., Bellmann, B., Takenaka, S., and Ziem, U. 1987. Inhalation and injection experiments in rats to test the carcinogenicity of MMMF. *Ann. Occup. Hyg.* 31(4B):755–764.
- Mumpton, F. A., and Thompson, C. S. 1975. Mineralogy and origin of the Coalinga asbestos deposit. *Clays Clay Miner.* 23:131–143.

- Oberdorster, G. 1995. Lung particle overload: Implications for occupational exposures to particles. *Regul. Toxicol. Pharmacol.* 21(1):123–135.
- Pooley, F. 2003. Personal communication of a report prepared under contract to KCAC of the examination of chrysotile asbestos samples from the asbestos mine and processing plant of KCAC, Inc., 1991.
- Reimschuessel, G. P. 1969. Unpublished information, Johns-Manville Research & Engineering Center, Manville, N.J. Cited by Speil and Leineweber (1969).
- Rogers, R. A., Antonini, J. M., Brismar, H., Lai, J., Hesterberg, T. W., Oldmixon, E. H., Thevenaz, P., and Brain, J. D. 1999. In situ microscopic analysis of asbestos and synthetic vitreous fibers retained in hamster lungs following inhalation. *Environ. Health Perspect.* 107(5):367–375.
- Speil, S., and Leineweber, J. P. 1969. Asbestos minerals in modern technology. *Environ. Res.* 2(3):166–208.
- Stoerber, W., Flachsbart, H., and Hochrainer, D. 1970. Der Aerodynamische Durchmesser von Latexaggregaten und Asbestfassern. *Staub-Reinh. Luft.* 30:277–285.
- U.S. Environmental Protection Agency. 2003. Report on the Peer Consultation Workshop to discuss a proposed protocol to assess asbestos-related risk. Prepared for U.S. Environmental Protection Agency, Office of Solid Waste and Emergency Response, Washington, DC 20460, EPA contract 68-C-98-148, Work Assignment 2003–05. Prepared by Eastern Research Group, Inc., Lexington, MA. Final Report May 30.
- World Health Organization. 1997. *Determination of airborne fibre number concentrations. A recommended method, by phase-contrast optical microscopy (membrane filter method)*. Geneva: World Health Organization.

APPENDICIX

The severity of histologic changes was scored minimal, slight, moderate, marked, and massive (grades 1–5, respectively) A score of zero indicates that this finding was not observed.

The tables presenting the degree of cellular lesions and fibrosis results in the initial publication (Bernstein et al., 2003) presented the means of only animals with a non-zero positive response as initially reported by the pathologist. This was not considered to be a true indicator of the group mean. This has been corrected with the mean values in Table 6 and Tables A1–A6, showing the group mean of all animals including those with no response (zero).

TABLE A1
Summary incidence of histopathological findings, 1 day after cessation of exposure

	Air control	Calidria chrysotile	Tremolite
Number animals per dose group examined	3	5	5
Lung			
Alveolar histiocytosis: reactive; focal/multifocal			
Grade 2	—	—	3
Grade 3	—	—	2
Number of animals affected	—	—	5
Mean total severity	—	—	2.4
Granuloma: bronchiolo—alveolar junction			
Grade 2	—	—	2
Grade 3	—	—	3
Number of animals affected	—	—	5
Mean total severity	—	—	2.6
Alveolar lining cell hypertrophy/hyperplasia			
Grade 2	—	—	1
Grade 3	—	—	1
Number of animals affected	—	—	2
Mean total severity	—	—	1.0
Bronchiolitis			
Grade 1	—	—	1
Grade 2	—	—	3
Number of animals affected	—	—	4
Mean total severity	—	—	1.4

TABLE A2
Summary incidence of histopathological findings, 2 days after cessation of exposure

	Air control	Calidria chrysotile	Tremolite
Number animals per dose group examined	3	5	5
Lung			
Alveolar histiocytosis: reactive; focal/multifocal			
Grade 3	—	—	5
Number of animals affected	—	—	5
Mean total severity	—	—	3.0
Granuloma: bronchiolo–alveolar junction			
Grade 3	—	—	5
Number of animals affected	—	—	5
Mean total severity	—	—	3.0
Alveolar lining cell hypertrophy/hyperplasia			
Grade 2	—	—	5
Number of animals affected	—	—	5
Mean total severity	—	—	2.0
Bronchiolitis			
Grade 2	—	—	4
Grade 3	—	—	1
Number of animals affected	—	—	5
Mean total severity	—	—	2.2
Alveolar hemorrhage			
Grade 2	—	1	—
Number of animals affected	—	1	—
Mean total severity	—	0.4	—

TABLE A3
Summary incidence of histopathological findings, 14 days after cessation of exposure

	Air control	Calidria chrysotile	Tremolite
Number animals per dose group examined	3	5	5
Lung			
Alveolar histiocytosis: reactive; focal/multifocal			
Grade 2	—	—	2
Grade 3	—	—	3
Number of animals affected	—	—	5
Mean total severity	—	—	2.6
Foam cell aggregation: focal/multifocal			
Grade 2	—	1	—
Grade 3	—	1	—
Number of animals affected	—	2	—
Mean total severity	—	1.5	—
Granuloma: bronchiolo–alveolar junction			
Grade 3	—	—	5
Number of animals affected	—	—	5
Mean total severity	—	—	3.0
Multinucleated giant cells in granulomas			
Grade 2	—	—	2
Number of animals affected	—	—	2
Mean total severity	—	—	1.0
Lungs, Trichrome			
Fibrosis in granulomas			
Grade 1	—	—	3
Grade 2	—	—	1
Number of animals affected	—	—	4
Mean total severity	—	—	1.0

TABLE A4
Summary incidence of histopathological findings, 90 days after cessation of exposure

	Air control	Calidria chrysotile	Tremolite
Number animals per dose group examined	3	4	4
Lung			
Alveolar histiocytosis: reactive; focal/multifocal			
Grade 2	—	—	1
Number of animals affected	—	—	1
Mean total severity	—	—	0.5
Foam cell aggregation: focal/multifocal			
Grade 2	—	2	—
Number of animals affected	—	2	—
Mean total severity	—	1.0	—
Granuloma: bronchiolo–alveolar junction			
Grade 2	—	—	1
Grade 3	—	—	3
Number of animals affected	—	—	4
Mean total severity	—	—	2.8
Lungs, trichrome			
Fibrosis in granulomas			
Grade 2	—	—	1
Grade 3	—	—	3
Number of animals affected	—	—	4
Mean total severity	—	—	2.8
Interstitial fibrosis			
Grade 2	—	—	1
Number of animals affected	—	—	1
Mean total severity	—	—	0.5
Mediast. lymph node			
Histiocytosis			
Grade 3	—	—	1
Number of animals affected	—	—	1
Mean total severity	—	—	0.75
Erythrophagocytosis			
Grade 2	—	—	1
Number of animals affected	—	—	1
Mean total severity	—	—	0.5

TABLE A5
Summary incidence of histopathological findings, 180 days after cessation of exposure

	Air control	Calidria chrysotile	Tremolite
Number animals per dose group examined	3	4	4
Lung			
Alveolar histiocytosis: reactive; focal/multifocal			
Grade 2	—	—	4
Number of animals affected	—	—	4
Mean total severity	—	—	2.0
Foam cell aggregation: focal/multifocal			
Grade 2	—	1	—
Grade 3	1	—	—
Number of animals affected	1	1	—
Mean total severity	0.75	0.5	—

TABLE A5
Summary incidence of histopathological findings, 180 days after cessation of exposure (*Continued*)

	Air control	Calidria chrysotile	Tremolite
Granuloma: bronchiolo–alveolar junction			
Grade 2	—	—	2
Grade 3	—	—	2
Number of animals affected	—	—	4
Mean total severity	—	—	2.5
Alveolar hemorrhage			
Grade 3	1	—	—
Number of animals affected	1	—	—
Mean total severity	0.25	—	—
Lungs, trichrome			
Fibrosis in granulomas			
Grade 1	—	—	1
Grade 2	—	—	3
Number of animals affected	—	—	4
Mean total severity	—	—	1.8
Interstitial fibrosis			
Grade 2	—	—	1
Number of animals affected	—	—	1
Mean total severity	—	—	0.50
Mediast. lymph node			
Erythrophagocytosis			
Grade 2	1	1	1
Number of animals affected	1	1	1
Mean total severity	0.5	0.5	0.5

TABLE A6
Summary incidence of histopathological findings, 365 days after cessation of exposure

	Air control	Calidria chrysotile	Tremolite
Number animals per dose group examined	4	4	4
Lung			
Foam cell aggregation: focal/multifocal			
Grade 1	1	—	—
Grade 2	2	1	—
Number of animals affected	3	1	—
Mean total severity	1.25	0.5	—
Granuloma: bronchiolo–alveolar junction			
Grade 1	—	—	3
Number of animals affected	—	—	3
Mean total severity	—	—	0.75
Alveolar hemorrhage			
Grade 1	1	—	—
Number of animals affected	1	—	—
Mean total severity	0.25	—	—
Lungs, trichrome			
Fibrosis in granulomas			
Grade 1	—	—	2
Grade 2	—	—	1
Number of animals affected	—	—	3
Mean total severity	—	—	1.0
Mediast. lymph node			
Erythrophagocytosis			
Grade 3	—	—	1
Number of animals affected	—	—	1
Mean total severity	—	—	0.75